DECOMPOSITION OF METAL THIOSEMICARBAZONE COMPLEXES FROM AMINOPHENAZONE-THIOUREA LIGAND INTO HDA AS A CAPPING MOLECULE FOR ZnS, CdS AND HgS NANOPARTICLES

T. XABA*, B. W. MASINGA, M. J. MOLOTO
Department of Chemistry, Vaal University of Technology, P/Bag X021, Vanderbijlpark, South Africa

The thiourea derivatives have been applied in many fields since they are modifiable ligands and can be able to coordinate to metal centres. The aminophenazone-thiourea ligand and the complexes of zinc (II), cadmium (II), and mercury (II) from the thiourea derivative ligand have been prepared and characterized by elemental analysis, FTIR spectroscopy and thermogravimetric analysis/differential thermogravimetric (TGA/DTG). Significant changes were observed in the FTIR spectra of the metal complexes compared to the FTIR spectrum of the ligand. These complexes were thermolyzed in hexadecylamine to synthesize HDA-capped ZnS, CdS, and HgS nanoparticles by thermal decomposition at 160 °C. The absorption band edges for ZnS and HgS nanoparticles prepared were blue shifted compared to their bulk materials except that of the CdS nanoparticles which was red shifted to it bulk material XRD confirms the predominance of hexagonal phase for ZnS and HgS whereas the CdS nanoparticles exhibit cubic phase. The size and morphology of nanoparticles were also determined from the TEM which showed spherical shapes for ZnS and HgS whereas the CdS nanoparticles revealed rod-like shape nanoparticles. The average particle sizes were found to be 4.44±1.24, 5.71±1.26 and 15.21±4.14nm for ZnS, CdS, and HgS, respectively.

(Received July 19, 2016; Accepted November 12, 2016)

Keywords: Thiosemicarbazone, Metal complexes, Hexadecylamine (HDA), Metal sulphide, Nanoparticles.

1. Introduction

The study based on thiourea derivatives has recently received considerable attention due to their complexation capacity [1-4], adjustable bonding modes, and promising biological inferences [5]. Many transition metal complexes from these ligands containing sulfur as donor atoms have been reported in the past. They can be considered as useful chelating agents due to their ability to capture the metal ions into their coordination structures. They are known to possess biological activities such as antifungal [6,7], antibacterial [8-10], antitumour [11], and pharmacological processes [12]. They can also be used in analytical chemistry to trace the platinum metals in complex matrices [13]. The metal thiosemicarbazone complexes have been confirmed as successful single source precursors for the synthesis of metal sulfide nanoparticles respectively [14,15].

The group IIB transition metal chalcogenides are important semiconductor compounds that have attracted much attention due to their exceptional properties and wide range of potential applications [16]. ZnS is one of the most promising semiconductor nanomaterials that can be used optoelectronic device applications such as optical coatings, solid-state solar cell windows, electro-optic modulators, photoconductors, field-effect transistors, sensors, transductors, light-emitting applications, and photonic. Amongst all the IIB–VI semiconducting nanoparticles, CdS nanoparticles is the most studied substance and it also has great potential applications in photocatalysis, optoelectronic devices, solar cell panel and light emitting diode display devices [17-19]. Several methods have been developed and reported for the synthesis of metal sulfide

* Corresponding author: thokozanix@vut.ac.za

nanoparticles including hydrothermal process [20], micro-emulsion method [21], sol-gel method [22], chemical co-precipitation method [23], sonochemical method [24], microwave irradiation [25], solvothermal method [26], and single source precursor method [27].

In this paper, the thiosemicarbazone ligand and its Zn(II), Cd(II), and Hg(II) complexes were prepared and subsequently thermolysed using the thermal decomposition method to produce metal sulphide nanoparticles. The Zn(II), Cd(II), and Hg(II) thiosemicarbazone complexes were thermolyed individually in the presence of hexadecylamine, as a capping molecule, under the same synthetic conditions to investigate the properties of the metal sulfide nanoparticles produced.

2. Experimental

2.1 Materials

Aminophenazone, cadmium chloride heptahydrate 99% (Sigma-Aldrich), thiourea, zinc chloride, mercury chloride, hexadecylamine, methanol, ethanol, acetone, and toluene were reagents purchased from Merck chemicals and were all used without further purification.

2.2 Physical measurements

The elemental analysis was achievedthrough Leco-CHNS 932 analyzer. About 2.0 mg of sample was introduced into Ag capsule and was placed in a furnace, which was maintained at a temperature of 800 °C. The FTIR spectra of the prepared ligand and complexes were recorded on a Perkin Elmer Spectrum 100 FTIR spectrometer. Few milligrams of the powder sample was placed on a sample holder and the spectrum was then recorded. The thermal gravimetric analysis (TGA) and differential thermogravimetric (DTG) were performed with the TA instruments-SDT-2960 simultaneous analyser to check the stability of the complexes. Dry samples were placed in an alumina cup and heated from 30 to 800 °C at a heating rate of 20 °C min^{-1} in a nitrogen gas environment. The optical measurements and properties were carried out using an Analytikjena Specord 50 UV-Vis spectrophotometer. The particles were dispersed in toluene, and solution was placed in a quarts cuvettes with 1 cm path length. A Perkin Elmer, LS 5 Luminescence spectrometer was used to measure the photoluminescence/emission of the nanoparticles. The samples were also placed in a quartz cuvette (1 cm path length). Transmission electron microscopy was acquired on the Hitachi Jeol 100S operated at 80 keV. A drop of nanoparticles solution made by dissolving the powder in toluene was placed on a copper grid. XRD patterns of the synthesized powdered samples were obtained on a Phillips X'Pert materials research diffractometer using secondary monochromated Cu Kα radiation (λ = 1.54060 A°) at 40 kV/50mA. Measurements were then taken using a glancing angle of incidence detector at an angle of 2 for 2θ values over 10 to 80 in steps of 0.05 with a scan speed of 0.012.

2.3 Preparation of aminophenazone-thiourea ligand

The substituted thiourea ligand was prepared according to the literature [28,29] as shown in Scheme 1. Aminophenazone (1 mmol) in hot ethanolic (20 mL) was mixed with (20 mL) hot ethanolic solution of thiourea (1 mmol). The mixture was stirred for 2 hrs on a water bath at 70 °C. On cooling the contents to room temperature, the precipitate was separated out, filtered, washed with acetone and dried in a desiccator. The ligand was obtained as white crystals. Percentage yield: 81%. M.pt. 45 °C. Anal. Calc. for [$C_{13}H_{19}SN_5$]: C, 56.29; H, 6.90; N, 25.25; S, 11.56. Found: C, 55.99; H, 6.71; N, 24.55; S, 11.48%. Significant IR bands: (cm^{-1}): ν(NH_2): 3361, ν(N–H): 3267, ν(C=N): 1581, ν(C–N): 1385, ν(N–N): 1079, ν(C=S): 949.

2.4 Preparation of the metal complexes

The preparation of all the metal complexes (Scheme 2) was performed by general procedure reported previously [30,31]. A hot solution of aminophenazone-thiourea ligand (0.256 g, 5 mmol) in ethanol (20 mL) was added to a heated solution of $CdCl_2.5H_2O$ (0.274 g, 5 mmol), $ZnCl_2$ (0.274 g, 5 mmol), $HgCl_2$ (0.274 g, 5 mmol) in ethanol (20 mL). The mixture was stirred and refluxed for 1 hr at a temperature of 70 °C. The colourless solution was filtered hot to remove

traces of unreacted materials and concentrate at room temperature. The coloured crystalline product was obtained after 24 hrs. The product was filtered, washed three times with ethanol and dried under vacuum.

2.4.1 Zinc complex

The complex was obtained as a white solid. Percentage yield: 47%. M.pt. 189 °C. Anal. Calc. for $[Zn(C_{13}H_{19}SN_5)_2Cl_2]$: C, 45.19; H, 5.54; N, 20.27; S, 9.28. Found: C, 45.27; H, 5.63; N, 19.95; S, 9.22%. Significant IR bands (cm^{-1}): ν(NH_2): 3358, ν(N–H): 3305, ν(C=N): 1628, ν(C–N): 1401, ν(N–N): 1029, ν(C=S): 954, ν(M-N): 539, ν(M-S): 484.

2.4.2 Cadmium complex

The complex was obtained as a cream white solid. Percentage yield: 77%. M.pt. 195 °C. Anal. Calc. for $[Cd(C_{13}H_{19}SN_5)_2Cl_2]$: C, 42.31; H, 5.19; N, 18.98; S, 8.68. Found: C, 41.99; H, 5.13; N, 19.05; S, 9.01%. Significant IR bands: (cm^{-1}): ν(NH_2): 3362, ν(N–H): 3287, ν(C=N): 1622, ν(C–N): 1406, ν(N–N): 1019, ν(C=S): 951, ν(M-N): 544, ν(M-S): 480.

2.4.3 Mercury complex

The complex was obtained as a black solid. Percentage yield: 69%. M.pt. 197 °C. Anal. Calc. for $[Hg(C_{13}H_{19}SN_5)_2Cl_2]$: C, 37.79; H, 4.64; N, 16.95; S, 7.76. Found: C, 38.05; H, 4.48; N, 16.52; S, 7.18%. Significant IR bands: (cm^{-1}): ν(NH_2): 3352, ν(N–H): 3276, ν(C=N): 1619, ν(C–N): 1403, ν(N–N): 1019, ν(C=S): 951, ν(M-N): 534, ν(M-S): 458.

2.5 Synthesis of the metal sulphide HDA capped nanoparticles

The metal sulphide nanoparticles were prepared from their respective metal complexes by thermal decomposition method. In a typical synthesis, the metal complexes (0.50 g) were each added into HDA (3 g) into a 250 mL three necked flask. The solid mixture was refluxed into an oil bath which was supported by a stirrer at 160 °C for an hour. After completion, the reaction mixture was allowed to cool to 70 °C and methanol was added to precipitate the nanoparticles. The solid was then separated by a centrifuge and washed three times with methanol. The resulting solid precipitates of HDA-capped MS nanoparticles were dispersed in toluene for further analysis.

3. Results and Discussion

The ligand based on thiosemicarbazone was synthesized using a simple and shorter method and reacted with metals such as Zn, Cd and Hg to form complexes. Their complexes were used as precursors for the synthesis of MS nanoparticles. Thermolysis was performed in HDA, at 160 °C for 1 hour to produce colourful ZnS, CdS and HgS nanoparticles. The complexes were characterized by elemental analysis which confirmed the elemental and structural composition of the complex and the FTIR spectra.

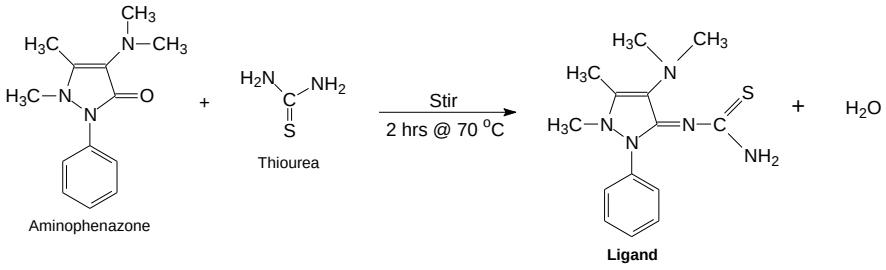

Scheme 1: Preparation of aminophenazone-thiourea ligand

The characteristic stretching vibration modes concerning the ligand and its metal complexes were investigated confirming the bidentate nature of the ligand to the complex. It also reveals that the bonding of the metals into the ligand is coordinated through N and S of the

thiourea group. The strong and high intensive bands from the ligand and metal complexes spectra were observed in the 3376, 3358, 3362 and 3352 cm^{-1} which are attributed to NH_2 vibrations. The strong absorption peaks at 1581, 1628, 1622, and 1619 cm^{-1} in a free ligand and in it metal complexes can be attributed to (C=N) stretching vibration of the bonding bridge between the thiourea and aminophenazone. The strong bands of the metal complexes which are due to the stretching of C–N groups are found at 1401, 1406, and 1403 cm^{-1} with higher frequencies (i.e. blue shifted) compared to the free ligand which absorbed at 1385 cm^{-1} which is an indication of the bidentate bonding behaviour of the ligand [32]. The adsorption peaks at 1079, 1029, and 1019 cm^{-1} were associated with N–N stretching vibrations from the aminophenazone ring. The high intensive absorption bands found from 949 to 954 cm^{-1} region are corresponding to the C=S vibrations which show the typical coordination between the ligand and the metal cations through sulphur and nitrogen atoms [32-34]. The FTIR results showed the new absorption bands at 539, 544, and 534 cm^{-1} which do not exist in the ligand spectrum that are attributed to M–N while the bands at 484, 480, and 458 cm^{-1} correspond to M–S which are the evidence for the coordination of metal to sulfur. This performance may be attributed to the electron discharging of the amines, which forces high electron density towards the sulfur atoms [35].

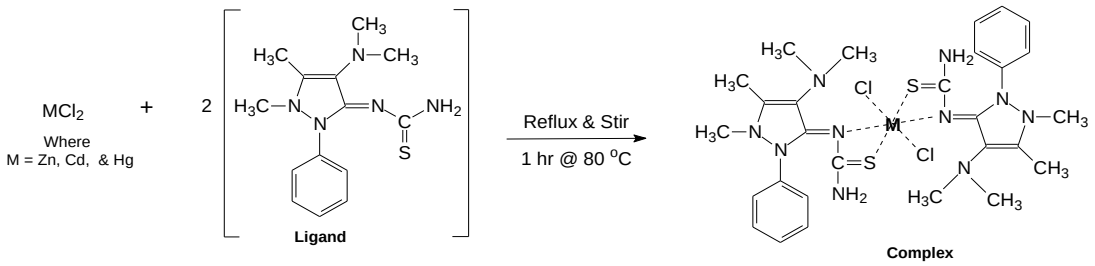

Scheme 2: Preparation of the metal (M = Zn, Cd or Hg) complexes

The thermal properties of the metal complexes were studied by thermogravimetric analysis at the temperature range from 20 to 800 °C under nitrogen atmosphere. Figure 1 shows the resulting TGA/DTG behaviour of the zinc, cadmium, and mercury complexes. The TGA/DTG in Figure 1(a) shows that zinc complex start to decompose at 190 °C and the weight loss happens in the temperature range of 190-426 °C. The weight loss may be attributed to the decomposition of the zinc complex with the weight loss of about 77%. In the case of cadmium complex, the TGA/DTG curves show three thermal decomposition stages which occur in 200-758 °C temperature range with a corresponding weight loss 70%. Figure 1(b) shows the first decomposition at 200-273 °C temperature range which may be attributed to the loss of C-N and C-C bonds from Aminophenazone-thiourea ligand. The second decomposition comes shortly after the first decomposition at a temperature of 292-353 °C which corresponds to about 10% weight loss. The third decomposition occurs in 575-758 °C temperature range, leaving a very low percentage of a residue. The TGA/DTG curves of mercury complex in Figure 1(c) were similar to the cadmium complex curves since its decomposition occurs in three consecutive stages as well which occurs at temperature between 200-730 °C. The first and second thermal decomposition stages are at 200-268 °C and 345-463 °C with the corresponding weight losses occurs through a very fast process due to combustion effect with the weight losses corresponding to 45% and 53% respectively. The third decomposition stage occurs at 650-730 °C with a weight loss that occurs very slowly.

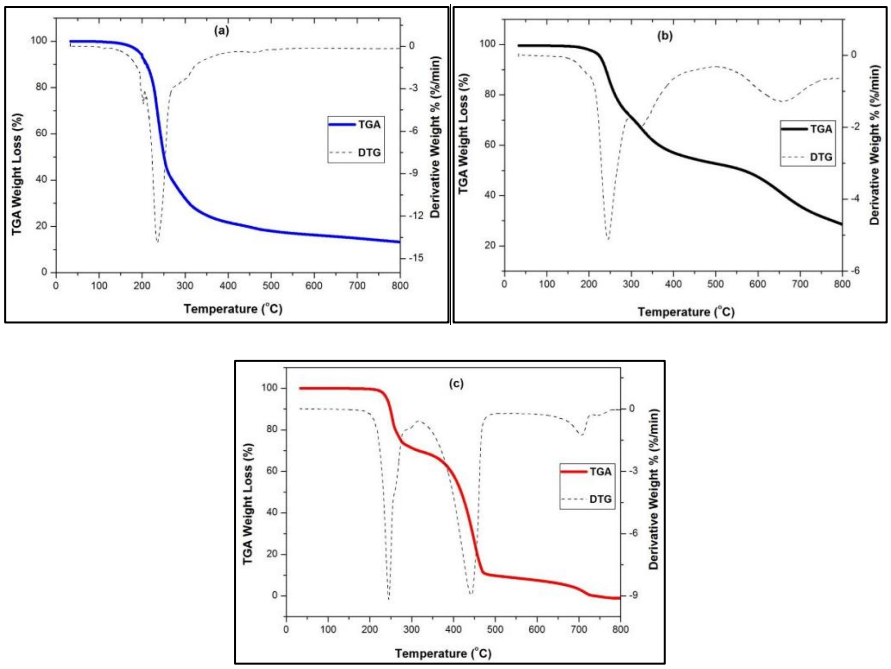

Fig. 1. TGA and DTG curves for zinc (a), cadmium (b), and mercury (c) complexes from aminophenazone-thiourea ligand.

The resultant metal sulfide nanoparticles were dispersed in toluene and the ultrasonic bath was used to speed up the dissociation of the particles in order to obtain better particle dispersions. The absorption studies of the metal nanoparticles were studied at room temperature in the region 250–800 nm. According to quantum confinement theory, the electrons in the conduction band as well as holes in the valence band are confined by the potential barrier of the surface. Due to this confinement of electrons and holes, the lowest energy optical transition from the valence to conduction band will increase in energy, effectively increasing the band gap (E_g) [33]. Either the shoulder or the peak of the spectra that is corresponding to the fundamental absorption edges in the samples can be used to estimate the band gap of the nanomaterial [36]. Figure 2 shows the UV-Vis spectra for HDA-capped ZnS, CdS, and HgS nanoparticles prepared at 160 °C from their respective metal complexes. ZnS and HgS gave absorption band edges with the largest blue shifts as compared to their bulk materials which are at 340 and 563 nm. The absorption spectra gave absorption peaks at 284 (4.37 eV) and 330 (3.76 eV) nm for ZnS and HgS. However, the band edge for CdS nanoparticles was observed at 520 (2.38 eV) nm which is red shifted relative to CdS bulk material, 515 nm which is an indication of the presence of rod shaped nanoparticles [37,38].

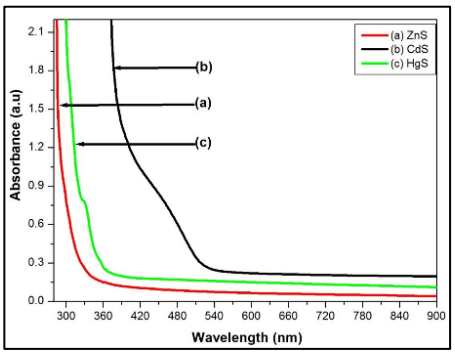

Fig. 2. UV-Vis spectra of HDA-capped ZnS (a), CdS (b) and HgS (c) nanoparticles.

Photoluminescence (PL) properties of HDA-capped ZnS, CdS and HgS nanoparticles prepared at 160 °C were also studied at room temperature with excitation at 260 nm (4.77 eV). Figure 3 shows the emission spectra of the metal sulfide nanoparticles with the emission maxima 337 (3.68 eV), 589 (2.11 eV), and 353 (3.51 eV) nm for ZnS, CdS and HgS, respectively. All the metal sulphide nanoparticles exhibit the well-defined absorption features. Among the three nanomaterials, only the ZnS and HgS are blue-shifted relative to their bulk materials except CdS which is red shifted to it bulk material.

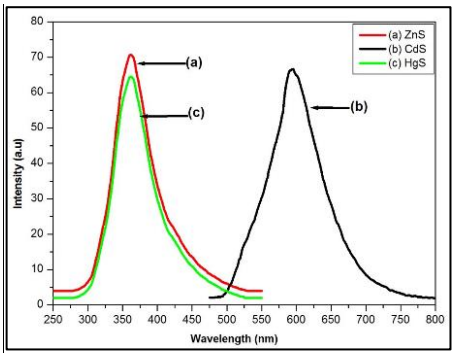

Fig. 3. Photolumniscence spectra of HDA-capped ZnS (a), CdS (b) and HgS (c) nanoparticles

The XRD patterns for the HDA-capped ZnS, CdS, and HgS nanoparticles synthesised at 160 °C are shown in Fig. 4. ZnS nanoparticles (Fig. 4(a)) is mainly exhibiting peaks at 22.28° (100), 24.08° (002), 25.06° (101), 30.58° (111), 39.76° (102), and 45.90° (110) which are the reflections of the hexagonal phase with lattice constants according to the literature (JCPDS card, No. 77-2306). Fig. 4(b) shows the XRD patterns of CdS nanoparticles, with three peaks observed at 2θ values of 30.42°, 51.18°, and 61.22° corresponding to the three crystal planes of (111), (220), and (311) of the cubic phase (JCPDS card, No. 05–0566). HgS nanoparticles (Fig.4(c)) gave predominantly broad peaks located at 30.42°(111), 35.00° (200), 50.88° (220), 60.62° (311), and 61.38° (222) for a hexagonal phase (JCPDS card, No. 00-006-0261).

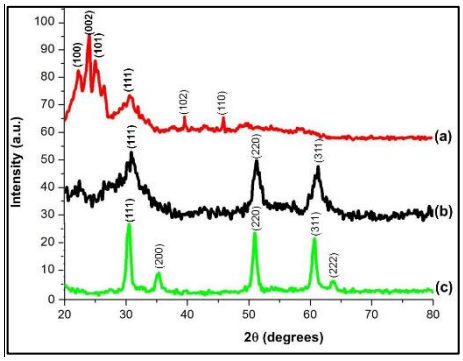

Fig. 4. X-ray diffraction patterns of HDA-capped ZnS (a), CdS (b) and HgS (c) nanoparticles.

TEM images of HDA-capped ZnS, CdS, and HgS nanoparticles prepared at 160 °C are displayed in Fig. 5. ZnS nanoparticles in Figure 5(a) revealed the dot shaped particles that are evenly distributed in morphology with an average particle size of 4.44±1.24 nm. Figure 5(b) shows rod-like shaped nanoparticles of CdS nanoparticles with the average particle size of 5.71±1.26 nm. HgS nanoparticles (Figure 5(c)) gave monodispersed spherical particles with the average size of 15.21±4.14 nm.

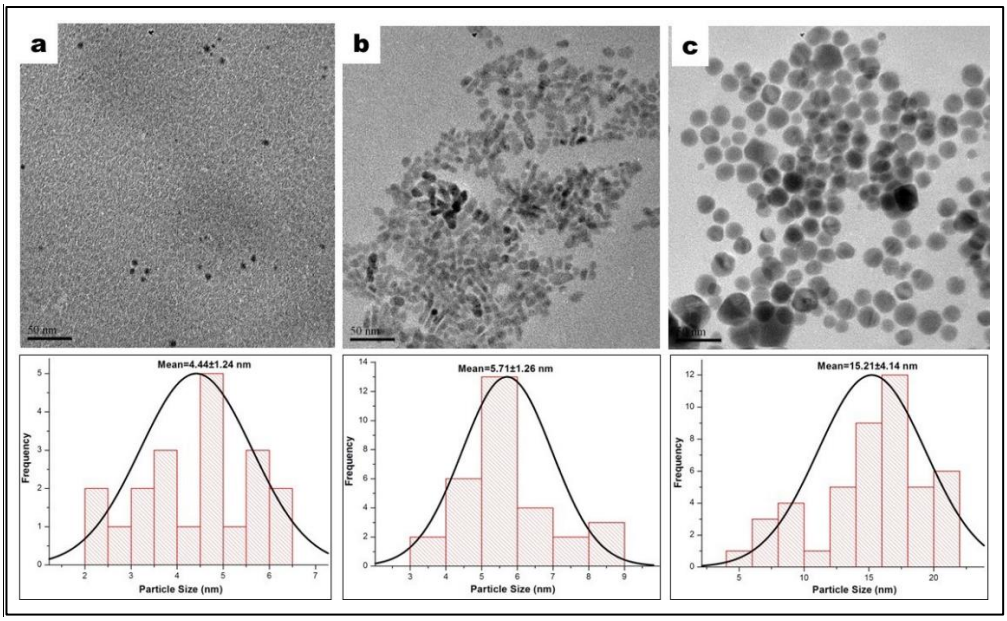

Fig. 5: TEM images of HDA-capped ZnS (a), CdS (b) and HgS (c) nanoparticles.

4. Conclusions

The thiourea derivative ligand and the complexes of Zn(II), Cd(II), and Hg(II) have been prepared and characterized by elemental analysis and spectroscopic techniques. The complexes were used to synthesize HDA capped ZnS, CdS, and HgS semiconductor nanoparticles. The complexes were thermolysed using the thermal decomposition method to yield nanoparticles with blue shifts in their absorption band edges by nm Stoke shifts.

The emission peaks are typically red shifted to the bulk materials by more than 10 nm. The Zn(II) and Hg(II) complexes produced particles of uniform size and spherical shapes that are highly monodispersed and hexagonal phases, driven by hexadecylamine. Cd(II) complex produced rod-like particles with the cubic phase.

Acknowledgements

The authors would like to thank the National Research Foundation (NRF) and the Vaal University of Technology, South Africa for their financial support.

References

[1] C. Y. Panicker, H. T. Varghese, A. George, P. K. V. Thomas, European Journal of Chemistry **1**, 173, 2010.
[2] J. R. Sabino, S. Cunha, R. M. Bastos, I. Vencato, Acta Crystallographica E **62**, 3918 (2006).
[3] T. Yesilkaynak, G. Binzet, F. M. Emen, U. Flörke, N. Külcü,H. Arslan, European Journal of Chemistry **1**, 1 (2010).
[4] K. H. König, M. Schuster, B. Steinbrech, G. Schneeweis, R. Schodder, Fresenius' Zeitschriftfür Analytische Chemie **321**, 457 (1985).
[5] G. M. Hossain, M. Abedin, S.C. Bachar, Organic Chemistry International **2012**, 1 (2012).
[6] R. Del Campo, J. J. Criado, R. Gheorghe, F. J. González, M. R. Hermosa, F. Sanz, J. L. Manzano, E. Monte, E. Rodrıguez- Fernández, Journal of Inorganic Biochemistry **98**, 1307 (2004).

[7] R. Del Campo, J. J. Criado, E. García, F. J. González, M. R. Hermosa, F. Sanz, J. L. Manzano,
E. Monte, E. Rodrıguez- Fernández, Journal of Inorganic Biochemistry **89**, 74 (2002).
[8] G. Binzet, H. Arslan, U. Flörke, N. Külcü, N. Duran, Journal of Coordination Chemistry, **59**, 1395 (2006).
[9] M. F. Emen, H. Arslan, N. Külcü,U. Flörke, and N. Duran, Polish Journal of Chemistry **79**, 1615 (2005).
[10] S. Saeed, N. Rashid, M. Ali, R. Hussain, European Journal of Chemistry **1**, 200 (2010).
[11] C. Sacht, M. S. Datt, Polyhedron **19**, 1347 (2000).
[12] S. Saeed, N. Rashid, M. Ali, R. Hussain, P.G. Jones, European Journal of Chemistry **1**, 221 (2010).
[13] O. A. Hassan, A. M. O. Abeer, National Journal of Chemistry **31**, 501 (2008).
[14] N. Srinivasan, S. Thirumaran, Superlattices and Microstructures **51**, 912 (2012).
[15] D. C. Onwudiwe, P. A. Ajibade, Int. J. Mol. Sci. **13**, 9502 (2012).
[16] M. R. Hoffmann, S. T. Martin, W. Y. Choi,D. W. Bahnemann, Chem Rev. **95**, 69 (1995).
[17] M. Matsumura, S. Furukawa, Y. Saho, H. J. Tsubomura, J. Phys Chem **89**, 1327 (1985).
[18] L. A. Silva, S. Y. Ryu, J. Choi, W. Choi, M. R. J. Hoffmann, J. Phys Chem C **112**, 12069 (2008).
[19] M. O. Melo, L. A. J. Silva, Photochem Photobio A: Chem **226**, 36 (2011).
[20] R. Maity, U. N. Maiti, M. K. Mitra, K. K. Chattopadhyay, Physica E **33**, 104 (2006).
[21] X. Cheng, Q. Zhao, Y. Yang, S. C. Tjong, R. K. Y. Li, J. Mater. Sci. **45**, 777 (2010).
[22] J. L. Yuan, K. Kajiyoshi, K. Yanagisawa, H. Sasaoka,K. Nishimura, Material Lett. **60**, 1284 (2006).
[23] I. Shafiq, A. Sharif,L.C. Sing, Physica E **41**, 739 (2009).
[24] X. H. Liao, J. J. Zhu,H. Y. Chen, Mater. Sci. Eng.B **85**, 85 (2001).
[25] J. J. Zhu, M. Zhou, J. Xu,X. Liao, Material Letters **47**, 25 (2001).
[26] Q. Zhao, L. Hou, R. Huang, Inorg. Chem. Commun. **6**, 971 (2003).
[27] T. Trindade, P. O'Brien, M. Zhang, Chem. Mater. **9**, 523 (1997).
[28] T. Xaba, M .J. Moloto, N. Moloto, Materials Letters, **146**, 91 (2015).
[29] A. Terol, A. Chauvet, G. De Maury, J. Masse, Farmaco Prat. **42**, 3 (1987).
[30] R. K. Agarwal, L. Singh, D. Kumar Sharma, Bioinorganic Chemistry and Applications **2006**, 1 (2005).
[31] P. Deshmukh, P. Kumar Soni, A. Kankoriya, A. K. Halve, R. Dixit, Int. J. Pharm. Sci. Rev. Res. **34**, 162 (2005).
[32] H. S. Sangari, G. S. SodhiI, J. Kaur, Chem. **51**, 280 (1997).
[33] D. C. Onwudiwe, P. A. Ajibade, Int. J. Mol. Sci. **12**, 5538 (2011).
[34] M. Lalia-Kantouri, M. Uddin, C. C. Hadjikostas, H. Papanikolas, G. Palios, S. Anagnostis, V. Anesti, Z. Anorg.Allg. Chem. **623**, 1983 (1997).
[35] I. Raya, I. Baba, B. M. Yamin, Malaysia. J. Anal. Sci. **10**, 93 (2006).
[36] T. T. Q. Hoa, L. V. Vu, T. D. Canh, N. N. Long, J. Phys. **187**, 12081 (2009).
[37] W. Xu, Y. Wang, R. Xu, S. Liang, G. Zhang, D. Yin, Journal of Materials Science **42**, 6942 (2007).
[38] R. John, S. F. Sasi, Chalcogenide Letters **7**, 269 (2010).